INTIMA MEDIA SEGMENTATION OF THE CAROTID ARTERY

C.P. Loizou [*], C.S. Pattichis [**], R.S.H. Istepanian [***], M. Pantziaris [****], T. Tyllis [****] and A. Nicolaides[****]

[*]Dep. of Computer Science, Intercollege, P. O. Box 51604, CY-3507 Limassol, Cyprus
[**] Dep. of Computer Science, University of Cyprus
[***]Mobile Information and Network Technologies Research Center (MINT@K), School of Computing and Information Systems, Kingston University, UK
[****]Cyprus Institute of Neurology and Genetics, Nicosia, Cyprus

E-Mail Address: christosl@lim.Intercollege.ac.cy

Abstract: In this study we present a new automatic segmentation technique for detecting the intima-media layer of the far wall of the common carotid artery in longitudinal ultrasound images, by applying snakes after image normalization and despeckling. We have tested and validated our segmentation technique on 100 images using the visual interpretation results and manual measurements by two vascular specialists. Results showed that no significant difference was found between the manual and the automatic segmentation measurements. Better segmentation results were obtained for the normalized despeckled images.

Introduction

The intima media thickness (IMT) of the common carotid artery (CCA) can serve as an early indicator of the development of cardiovascular disease, like myocardial infraction and stroke [1]. Previous studies indicated that increase in the IMT of the CCA is directly associated with an increased risk of myocardial infraction and stroke [1]-[3]. Traditionally, the IMT is measured by manual delineation of the intima and the adventitia layer. The manual tracing method is not only tedious and time consuming, but also suffers from inter- and intra-observer variability. The objective of this study is to evaluate an automated IMT segmentation method using snakes.

Various computerized methods have been developed for vascular or intra-vascular ultrasound segmentation of the IMT. A deformable model for 3D real world images was proposed in [4]. Cohen [5] proposed a balloon model for the snake, in 2D US images of the heart by using the finite element method to calculate the function of continuity. In [6] an energy minimization process was developed, based on the snake model, where the energy function was composed of three terms, a continuity term, a curvature term and an image term. A computerized analysis system to automatically extract the boundaries of the IMT using dynamic programming in longitudinal 2D images of the carotid artery was proposed in [2]. Deformable models for 3D transversal images were used in [1], by providing a seed point in the lumen of the carotid artery. Cheng [3] proposed an automatic system for detecting the IMT in 2D longitudinal images of the carotid artery based on the active contour model. Mao [7] proposed a deformable discrete dynamic contour model in transversal 2D images of the carotid artery, with only one seed point to guide the initialization of the deformable model.

Most of the proposed techniques have certain limitations: 1) They require manual correction after automatic tracing [2], [3]. 2) They are sensible to the initial snake contour [3], which should be placed manually [1]. If the initial contour is placed far away from the object of interest then the snake will not be attracted [3]. 3) They do not take into consideration the speckle noise in the ultrasound image as well as they have not been evaluated on a significant number of images, where the intra- and inter-observer variability [8] could not be assessed. 4) Some weighting factors must be entered manually [5] and have difficulties processing concave boundary regions [6].

In the following Section the procedure of recording the ultrasound images, the manual measurements of IMT, image normalization, despeckling, snake segmentation, as well as a set of evaluation metrics are described. In the Results Section the results of the segmentation technique are described and finally in the last Section the concluding remarks are presented.

Materials and Methods

A. Recording of Ultrasound Images

A total of 100 ultrasound images of the carotid artery were acquired using the ATL HDI-5000 ultrasound scanner [8]. They were recorded digitally on a magneto optical drive, with a resolution of 768x756 pixels with 256 gray levels. The image resolution was 16.66 pixels/mm.

B. Manual Measurements of IMT

Two vascular specialists delineated the IMT on all 100 ultrasound images of the carotid artery before and after image normalization (see next subsection), by selecting 10 consecutive points for the adventitia and the intima at the far wall of the carotid artery. The measurements were performed 1cm proximal to the bifurcation of the CCA at a length of 2-3 cm on the far wall. The IMT was calculated as the average of the 10

measurements. Measurements taken from the near wall are avoided because they are less accurate, caused by overlap of echo pulses, and therefore less reproducible than those taken from the far wall [9]. This is because the adventitia is more echogenic than the blood and bright echoes produced by the adventitia of the near wall can "spill" into the adjacent blood. Thus, echoes from the blood are lost.

C. Image Normalization

The images were normalized manually by linearly adjusting the image so that the median gray level value of the blood was 15-20, and the median gray level of the adventitia (artery wall) was 180-200 [10]. The scale of the gray level of the images ranged form 0-255. This normalization using blood and adventitia as reference points was necessary in order to extract comparable measurements in case of processing images obtained by different operators or different equipment [10].

D. Despeckling

Speckle is a form of multiplicative noise, which corrupts medical ultrasound imaging making visual observation difficult. Many researchers refer to speckle as the major difficulty in analyzing and segmenting US images [1]-[3], [7]. In a recent study [11] we have shown that despeckle filtering improves the optical perception of the physician.

In this study, the linear filter *lsmv* was used, which may be described by a weighted average calculation using sub region statistics to estimate statistical measures over 7x7 pixel windows [11]. The filter was applied 5 times iteratively on each image.

E. Snakes Segmentation

A snake contour may be represented parametrically by $v(s) = [x(s), y(s)]$, where $(x, y) \in \Re^2$ denote the spatial coordinates of an image and $s \in [0,1]$ represents the parametric domain. The snake adapts itself by a dynamic process that minimizes an energy function defined as [3]-[6]

$$E_{snake}(v(s)) = E_{\text{int}}(v(s)) + E_{image}(v(s)) + E_{ext}(v(s)) = \int_s (\alpha(s)E_{cont} + \beta(s)E_{curv} + \gamma(s)E_{image} + E_{external})ds \quad (1)$$

At each iteration step, the energy function is evaluated for the current point in $v(s)$, and for the points in an mxn neighborhood along the arc length s of the contour. Subsequently the point on $v(s)$ is moved to the new position in the neighborhood that gives the minimum energy. The term $E_{\text{int}}(v)$ in (1) denotes the internal energy derived from the physical characteristics of the snake and is given by the continuity $E_{cont}(v)$ and the curvature term $E_{curv}(v)$. It controls the natural behavior of the snake. The internal energy contains a first-order derivative controlled by $\alpha(s)$, which discourages stretching and makes the model behave like an elastic string by introducing tension and a second order term controlled by $\beta(s)$, which discourages bending and makes the model behave like a rigid rode by producing stiffness. The weighting parameters $\alpha(s)$ and $\beta(s)$ can be used to control the strength of the model's tension and stiffness, respectively. Altering the parameters α, β and γ, one may control the operation of the snake. The second term in (1) $E_{image}(v)$, represents the image energy due to some relevant features such as the gradient of edges, lines, regions [3] and texture [6]. It attracts the snake to low-level features such as brightness and edge data. Finally the term $E_{external}(v)$ is the external energy of the snake, which is user defined and optional. A modification of the greedy algorithm [6] was used in our study based on the principle of an energy minimizing spline as in (1).

It is importnat to place the initial snake contour as close as possible to the area of interest otherwise the snake may be trapped into local minima or false edges, and converge in a wrong location. We have therefore developed an initialization procedure as follows: a) Selelect the area where the intima media will be detected. b) Despeckle and convert the image to binary in order to extract edges more easily. c) Dilate the binary image and remove eroneous edges. d) Locate points on the adventitia and construct an interpolating B-spline. e) Map the points in the gray level image to construct the initial contour for the adventitia. f) Displace the contour upwards for upto 20 pixels (1.2mm) to detect the intima layer, based on the observation that the IMT lies between 0.6 mm and 1. 8 mm. g) Deform the initial contours by a snake to automatically detect the IMT borders. h) sample both contours at 30 consequtive snake points and i) Calculate and display the average minimum, maximum and median values for the IMT.

F. Evaluation Metrics

In order to investigate how the new automated method results differ from the manual delineation results, we used the following evaluation metrics

We computed the parameters IMT_{mean}, $IMT_{\min}$, $IMT_{\max}$ and IMT_{median}, as well as the inter-observer error according to the formula $s = \sigma_{IMT}/\sqrt{2}$. We also calculated the coefficient of variation ($CV\%$), which describes the difference as a percentage of the pooled mean value (IMT_{mean}) by using the formula, $CV\% = \frac{s * 100}{IMT_{mean}}$ [11].

The Wilcoxon rank sum test is used in order to identify if for each measurement a significant (S) difference or not (NS) exists between the computer-generated and the hand-outlined boundaries, at $p < 0.05$. Further the Hausdorff distance (HD) [12] between two curves was calculated. It reflects the maximum mismatch ($HD = |Manual - Automatic|$) between the manual and the automated boundaries. Small values for the HD are favorable. Also the Pearson correlation test was used, which returns the Pearson product moment correlation coefficient, r, that ranges from –1.0 to 1.0

inclusive and reflects the extent of a linear relationship between two data sets [12]. The mean-square error (MSE) between the computer generated and the hand-outlined boundaries was also calculated, which estimates the minimum average distance squared [11], between the two curves. Therefore small values for MSE are required.

The strength of the relationship between the automated and manual methods is indicated by the correlation $c_{m,a} = \frac{Cov_{m,a}}{\sigma_m \sigma_a}$, where $Cov_{m,a}$ is the covariance between the automated and the manual measurements and σ_m, σ_a are the standard deviation of the two measurements respectively [13]. Further, the correlation coefficient ρ was investigated to determine the relationship between the measurements.

Results

Figure 1 shows a longitudinal ultrasound image of the carotid artery with the manual delineations M, and MN from the two observers, the initial contour estimation, and the segmentation results for the cases of no filtering (NF), despeckled (DS), normalized (N), and normalized despeckled (ND) respectively. The best optical results as assessed by the two physicians were obtained on the normalized despeckled (NDS) image followed by the N and DS.

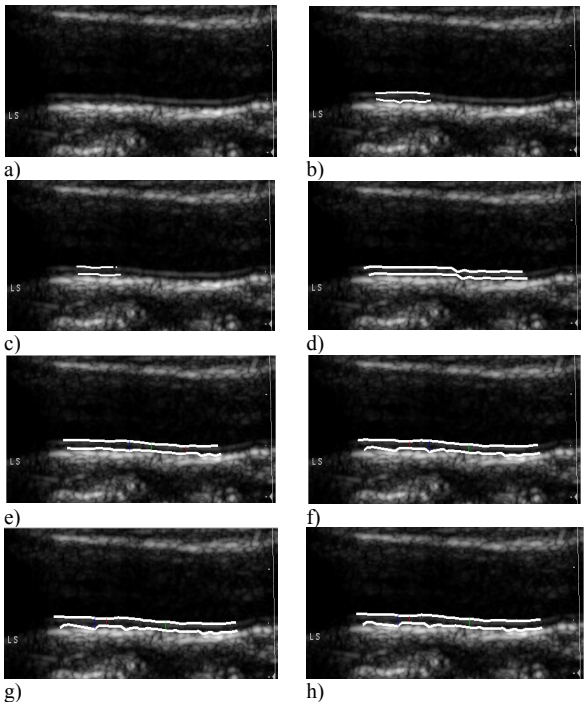

Figure 1: a) The original ultrasound image of the carotid artery, b) manual delineation from first expert, c) manual delineation from second expert, d) initial contour estimation, and the segmentation results of the IM for, e) no filtering (NF), f) despeckled (DS), g) normalized (N), and h) normalized despeckled (NDS) images

Table 1 tabulates the manual and automated results for 100 images, of the $IMT_{mean}, IMT_{\min}$, $IMT_{\max}$ and IMT_{median} with their standard deviations (sd), the inter observer error (s) and the coefficient of variation ($CV\%$). The IMT_{mean} values computed from the two experts were 0.67 and 0.65 mm, whereas for the segmented measurements were 0.70, 0.69, 0.67 and 0.68 mm for the NF, DS, N and NDS respectively. Best segmentation results are shown with bolded values and were obtained for the NDS images, with an sd of the IMT_{mean} of 0.12, an s of 0.08 and a $CV\%$ of 12.5% respectively.

Table 2 shows the results of the Wilcoxon rank sum test, the HD, the Pearson correlation and the MSE. The Wilcoxon rank sum test, which is displayed in the upper triangle of the left column of Table 2, shows that NS difference exists between the automated and manual measurements. The HD, which is displayed in the lower triangle of Table 2 shows that minimum mismatches were obtained between the N-M (3.4), NDS-MN (4.7), NDS-N (5.2), DS-NF (5.2), NDS-M and DS-MN (8.6) respectively. Higher Pearson correlation values were observed for the NF-DS (0.98), DS-N (0.95), NF-N (0.95), DS-NDS (0.92), and N-NDS (0.91) respectively. Low Pearson correlation values were observed between the M-NDS (0.63), MN-NDS (0.66), M-NF (0.67), M-DS (0.70), MN-NF (0.71), M-N (0.71), MN-DS (0.73) and MN-N (0.75) respectively. MSE results are given in the lower triangle of the right column. Low MSE values are observed for N-M (0.01), NDS-MN (0.02), NDS-N (0.03) and DS-NF (0.03) respectively.

Table 1: Comparison between manual and automated measurements for the 100 US images of the carotid artery. Measurements are in millimeters (mm). Bolded values show best performance

	Manual Measurements				Segmentation Measurements			
	Expert 1		Expert 2					
	M	MN	M	MN	NF	DS	N	NDS
IMT_{mean}	0.67	0.68	0.65	0.61	0.70	0.69	0.67	0.68
(sd)	(0.16)	(0.17)	(0.18)	(0.17)	(0.14)	(0.13)	(0.13)	(**0.12**)
IMT_{min}	0.53	0.52	0.57	0.54	0.51	0.51	0.50	0.49
(sd)	(0.14)	(0.15)	(0.16)	(0.14)	(0.13)	(0.13)	(0.14)	(**0.11**)
IMT_{max}	0.82	0.85	0.75	0.70	0.90	0.88	0.86	0.87
(sd)	(0.22)	(0.21)	(0.19)	(0.20)	(0.20)	(0.19)	0.17)	(**0.15**)
IMT_{median}	0.66	0.66	0.67	0.61	0.69	0.69	0.66	0.64
(sd)	(0.16)	(0.18)	(0.18)	(0.17)	(0.14)	(0.13)	(0.12)	(**0.12**)
s	0.11	0.12	0.13	0.11	0.10	0.09	0.09	**0.08**
CV %	16.7	17.1	19.1	17.2	13.8	13.4	13.2	**12.5**

M: Manual, MN: Manual normalized, NF: No filtering, DS: Despeckled, N: Normalized, NDS: Normalized despeckled, (sd): Standard deviation, s: Inter observer error for mean values, CV %: Coefficient of variation

Table 2: Tests and measures computed on 100 US images of the carotid artery. Left column upper triangle: Wilcoxon Rank Sum test (S=Significant differnce, NS=Non Significant differecne at $p<0.05$). Left column lower triangle: Hausdorff Distance ($*10^{-3}$). Right column upper triangle: Pearson Correlation test. Right column lower triangle: Mean-Square Error ($*10^{-3}$). Bolded values show best performance

	Wilcoxon Ranksum Test and HD						Pearson Correlation and MSE					
	M	MN	NF	DS	N	NDS	M	MN	NF	DS	N	NDS
M	-	NS	NS	NS	NS	NS	-	**0.90**	0.67	0.70	0.71	0.63
MN	13.3	-	NS	NS	NS	NS	0.20	-	0.71	0.73	0.75	0.66
NF	27.1	13.8	-	NS	NS	NS	0.70	0.20	-	**0.98**	**0.95**	**0.90**
DS	21.9	**8.6**	**5.2**	-	NS	NS	0.50	0.07	**0.03**	-	**0.95**	**0.92**
N	**3.4**	9.9	23.7	18.5	-	NS	**0.01**	0.09	0.60	0.40	-	**0.91**
NDS	**8.6**	**4.7**	18.5	13.3	**5.2**	-	0.07	**0.02**	0.40	0.20	**0.03**	-

Table 3 presents the results of the covariance and the correlation coefficient between the different methods. Higher correlation values were obtained for the cases, NF-DS (16.3), DS-N (14.4), NF-N (14.4), DS-NDS (13.1), N-NDS (12.9) and NF-NDS (12.8) respectively. In the right column of Table 3 higher values for the correlation coefficient were obtained for the cases, NF-DS (0.97), DS-N (0.93), NF-N (0.93), DS-NDS (0.92), N-NDS (0.91) and NF-NDS (0.90) respectively.

Table 3: Covariance ($c_{m,a}$) and Correlation coefficient ρ for the 100 US images of the carotid artery. Bolded values show best performance

	Covariance					Correlation Coefficient				
	MN	NF	DS	N	NDS	MN	NF	DS	N	NDS
M	**21.7**	10.7	10.4	9.8	9.1	0.88	0.59	0.62	0.63	0.63
MN		11.5	11.1	10.4	9.5		0.63	0.66	0.66	0.66
NF			**16.3**	**14.4**	**12.8**			**0.97**	**0.93**	**0.90**
DS				**14.4**	**13.1**				**0.93**	**0.92**
N					**12.9**					**0.91**

Conclusions

In this paper we proposed a new automated system for segmenting ultrasound images of the carotid artery by using snakes for the measurement of intima media thickness, which requires minimum user interaction.We have evaluated the method on 100 longitudinal ultrasound images of the carotid artery using optical perception evaluation by two experts, statistical measures, and error metrics.

The most important findings of our study are the following: (i) there is no significant difference for the measurement of IMT between the manual and the snakes segmentation measurements, and (ii) better segmentation results (smaller interobserver variability, and smaller coefficient of variation) were obtained for the normalized despeckled images.

The no significant difference between the manual and the automated method, shows that the manual method may be replaced by the automated method, thus the expert may carry out auotmated measurements reliably. The manual measurements are smaller than the automated and this finding was also reported in other studies [1]-[3].

Our method yielded smaller interobserver error, s, compared to other studies [1]-[3], [7] where higher values were reported. The coefficient of variation, $CV\%$, of this study when compared to other studies [2], [12], [13] was higher for the manual measurements, but lower for the automated measurements. In the studies reported above [1]-[3], [7], [12], [13], no despeckle filtering and normalisation were carried out. Moreover, initial contour estimation similar to our study was also performed in [1] and [3].

Concluding, the segmentation of the IMT in the carotid artery is more accurate and reproducible with the manual results, when performed on a normalized despeckled ultrasound image (NDS). Normalisation and despeckle filtering may be therefore successfully used, for the automated segmentation of ultrasound carotid images.

ACKNOWLEDGEMENTS

This work was partly funded through the project *Integrated System for the Support of the Diagnosis for the Risk of Stroke (IASIS),* of the 5th Annual Program for the Financing of Research of the Research Promotion Foundation of Cyprus.

References

[1] ZAHALKA A., FENSTER A. (2001): 'An Automated Segmentation Method for Three-Dimensional Carotid Ultrasound Images', *Phys. Med. Biol.* **46**, pp. 1321-1342

[2] LIANG Q., WENDELHAG I., WILKSTRAND J., GUSTAVSSON T. (2000): 'A Multiscale Dynamic Programming Procedure for Boundary Detection in Ultrasonic Artery Images', *IEEE Trans. Med. Imag.*, **19** (2), pp. 127-142

[3] CHENG D., SCHMIDT-TRUCKSAESS A., CHENG K., BURKHARDT H. (2002): 'Using Snakes to Detect the Intimal and Adventitial Layers of the Common Carotid Artery Wall in Sonographic Images', *Comp. Meth. Prog. in Biom.*, **67**, pp. 27-37

[4] TERZOPOULOS D., WITKIN A., KASS M. (1987): 'Symmetry-seeking models for 3-D object reconstruction', *Int. J. Comp. Vision*, **1** (3), pp. 211-221

[5] COHEN L. D. (1991): 'On Active Contour Models and Balloons', *Comp. Vis. Graph. Imag. Proc. Imag. Und.,* **53** (2), pp. 211-218

[6] WILLIAMS D. J., SHAH M. (1992): 'A fast algorithm for active contour and curvature estimation', GVCIP: Image Understanding, **55** (1), pp. 14-26

[7] MAO F., GILL J., DOWNEY D., FENSTER A. (2000): 'Segmentation of Carotid Artery in Ultrasound Images: Method Development and Evaluation Technique', *Med. Phys.* **27** (8), pp. 1-10

[8] A PHILIPS MEDICAL SYSTEM COMPANY (2001): 'Comparison of image clarity, SonoCT real-time compound imaging versus conventional 2D ultrasound imaging', ATL Ultrasound, Report

[9] PIGNOLI P., ET AL. (1986): 'Intima Plus Media Thickness of the Arterial Wall: A Direct Measurement with Ultrasound Imaging', *Atheroscler.*, **74** (6), pp. 1399-1406

[10] ELATROZY T., NICOLAIDES A., TEGOS T., ZARKA A., GRIFFIN M., SABETAI M. (1998): 'The Effect of B-mode ultrasonic image standardization of the echodensity of symptomatic and asymptomatic carotid bifurcation plaque', *Int. Angiol.*, **17** (3), pp. 179-186

[11] LOIZOU C., CHRISTODOULOU C., PATTICHIS C. S., ISTEPANIAN R., PANTZIARIS M., NICOLAIDES A. (2002): 'Speckle Reduction in Ultrasound Images of Atherosclerotic Carotid Plaque', DSP 2002, IEEE 14th Int. Conf. on Digital Signal Proc., **2**, pp. 525-528

[12] CHALANA V., KIM Y. (1997): 'A methodology for evaluation of boundary detection algorithms on medical images', *IEEE Trans. Med. Imag.,* **16** (5), pp. 642-652

[13] GUTIERREZ M., PILON P., LAGE S., KOPEL L., CARVALHO R., S. FURUIE (2002): 'Automatic measurement of carotid diameter and wall thickness in ultrasound images', *Comp. Cardiol.*, **29**, pp. 359-362.